



ELSEVIER

Contents lists available at ScienceDirect

Nuclear Instruments and Methods in Physics Research A

journal homepage: www.elsevier.com/locate/nima

Results from polarization studies of radio signals induced by cosmic rays at the Pierre Auger Observatory

H. Schoorlemmer

Nikhef and Institute of Mathematics, Astronomy and Particle Physics, Radboud University Nijmegen, The Netherlands

For the Pierre Auger Collaboration^{1,2}

ARTICLE INFO

Available online 10 December 2010

Keywords:

Pierre Auger Observatory
Cosmic ray
Radio detection
Coherent radio emission
Polarization
Charge-excess radiation

ABSTRACT

At the Pierre Auger Observatory, the radio emission from cosmic-ray-induced air showers is measured. We will discuss the physics results from a setup consisting of three antennas triggered by an auxiliary particle detector. With this setup, a total of 494 events were registered in coincidence with the surface detector of the Pierre Auger Observatory. This data allows us to study the dependence of the radio signal on air shower parameters. From an analysis of the measured polarization of the radio signals, we conclude that the emission is dominated by the geomagnetic mechanism. However, the polarization study indicates that the pure geomagnetic description by itself is not sufficient to describe all features of the data set.

© 2010 Elsevier B.V. All rights reserved.

1. Introduction

Cosmic-ray-induced extensive air showers (EAS) emit radiation in the MHz domain, that can be detected by antennas. This was first shown by Jelley in 1965 [1]. The radio-detection technique of EAS had a revival with experiments like CODALEMA [2] and LOPES [3]. At the Pierre Auger Observatory [4], a next generation radio detector is currently under construction: the Auger Engineering Radio Array (AERA) [5], a radio detector with a collecting area of $\sim 20 \text{ km}^2$. Several prototype setups have been operated in the past years at the Pierre Auger Observatory site. Although they were designed for testing purposes, these setups produce interesting physics results on their own.

The polarization of the radio signal is crucial to understand the emission mechanism(s) inducing the radio signal from EAS. In Refs. [6,7] it is shown that different contributions leading to the radio signal should have different polarization signatures. In this article we present a method to reveal contributions of different emission mechanisms by using the polarization of the radio signals.

2. Setup and data selection

The data used in this analysis was taken with a setup consisting of three antennas that were triggered by a scintillator particle detector [8]. The antennas, near the balloon launching station (BLS)

of the observatory, were positioned in a triangle and separated from each other by 100 m. This setup was operational in the period from May 2007 until May 2008. From the three antennas of the setup, only data from two logarithmic-periodic dipole antennas (LPDA) [9] are used in the analysis. At the other antenna location, several types of antennas were tested. The LPDA is a dual antenna, with one antenna polarized in the east–west (EW) direction and the other one polarized in the north–south (NS) direction. After a trigger both EW and NS directions were read out for a period of 10 μs with a sampling frequency of 400 MHz. These ADC time series of each polarization channel were written to disk.

In total there were 494 events triggered in coincidence with the surface detector (SD) from the Pierre Auger Observatory. For these events the EAS parameters reconstructed by the SD are used in this analysis.

Since not all events contain a radio signal that is significantly above the noise level, a signal-to-noise cut is applied to the data. This cut is defined on the time series of total measured power. These time series are obtained by adding the squared envelopes of the time series from the EW and NS channels. To find the signal in the times series the arrival time of the radio signal is predicted from the direction of the SD reconstructed event and a known offset. In a window, with a width of 300 ns and centered around the expected signal time, the position of the maximum is determined. Around this maximum a full width half maximum (FWHM) window is defined, in which the average power is calculated. Radio signals that have an average power in their FWHM window that is five times higher than the average power in a noise window (the first 750 samples from the time series) are used in the analysis. The FWHM window from the selected radio signals is used to define a signal window.

E-mail address: h.schoorlemmer@hef.ru.nl

¹ Av. San Martín Norte 304 (5613) Malargüe, Prov. de Mendoza, Argentina.

² A full author list and affiliations can be found at http://www.auger.org/archive/authors_2010_08.html.

At the BLS, there is a weather station operational equipped with an electric field monitor. It is known that thunderstorms can have impact on the radio signals from EAS [10]. Therefore, events measured during thunderstorms, or when the thunderstorm monitor was not operational, are rejected from the analysis. There are 38 radio signals that survive all selection cuts.

3. Results

3.1. Geomagnetic emission mechanism

The dominant contribution to radio signals from EAS is the result from coherent radiation due to deflection of charged particles from the EAS in the geomagnetic field. This geomagnetic emission mechanism was introduced by Kahn and Lerche [11] and has been verified by experiments such as LOPES and CODALEMA [12]. The polarization signature of geomagnetic radiation should be linear polarized in the direction perpendicular to the EAS axis and the geomagnetic field axis. The angle of linear polarization in the horizontal plane, ϕ_{mag} , can be calculated because the direction of the incoming shower is known from the reconstructed EAS from the SD

$$\phi_{\text{mag}} = \arctan\left(\frac{(\vec{A} \times \vec{B})_{\text{NS}}}{(\vec{A} \times \vec{B})_{\text{EW}}}\right). \quad (1)$$

In which \vec{A} is the shower axis pointing into the arrival direction of the EAS, and \vec{B} is the direction of the geomagnetic field. The uncertainty on ϕ_{mag} is obtained by propagation of the uncertainty on the shower axis. This uncertainty is $\sim 0.7^\circ$. The uncertainty in the orientation of the antenna leads to a systematic uncertainty on ϕ_{mag} , this is estimated to be $\sim 5^\circ$.

From the measurements, the angle of linear polarization can be calculated from the Stokes parameters (see for example Ref. [13])

$$\phi_i = \frac{1}{2} \arctan\left(\frac{U_i}{Q_i}\right) \quad (2)$$

where ϕ_i is the polarization angle and U_i and Q_i are the Stokes parameters³ defined for the i -th sample of the time series. To estimate the polarization angle over the radio pulse the average polarization angle, $\bar{\phi}$, is calculated over all samples within the signal window. The uncertainty on this parameter is calculated as

$$\Delta\bar{\phi} = \frac{K}{N} \sqrt{\sum_{i=1}^N (\phi_i - \bar{\phi})^2}. \quad (3)$$

The factor K is defined by the amount of oversampling $f_s/2\Delta f$, with Δf the sensitive band width of the setup, and f_s the sampling frequency. N is the number of samples in the signal window, and sample $i=1$ is defined as the lower edge of the signal window.

In Fig. 1, $\bar{\phi}$ is plotted against ϕ_{mag} for the selected radio signals. The data follows the expected trend for geomagnetic radiation.

3.2. Charge-excess

From theory it is expected that a secondary contribution to the radio pulse is due to variation of a negative charge-excess while the EAS propagates through the atmosphere [14]. Since the polarization of a radio signal depends on the relative strength of different contributions, the overall polarization cannot be calculated by a simple calculation. Therefore, the data will be compared to REAS3 [15] and MGMR [6] simulations, that both incorporate the charge-excess contribution. To compare the data with simulations the full

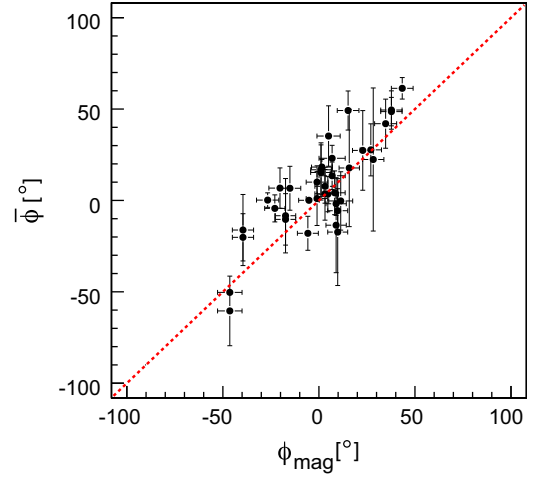


Fig. 1. The mean measured polarization angle versus the polarization angle expected from geomagnetic radiation. The dotted red line indicates the expectation for geomagnetic radiation. (For interpretation of the references to color in this figure legend, the reader is referred to the web version of this article.)

detector response is applied to the simulations. This is done with the radio part of the Auger Offline software package [16].

The charge-excess radiation has a different polarization signature than the geomagnetic radiation. The electric field is radially polarized around the EAS axis. This means that the direction of the polarization depends on the angle with respect to the observer in the plane perpendicular to the shower axis. We define this observer angle, ϕ_{obs} , as the angle with the east axis (positive towards north) in the plane perpendicular to the shower axis.

To compare the charge-excess polarization of different EAS to each other, a transformation is applied

$$\phi'_{\text{obs}} = \phi_{\text{obs}} - \phi_{\text{mag}}. \quad (4)$$

To define a parameter that is sensitive to deviations to a polarization from geomagnetic radiation, the two channels are rotated around ϕ_{mag} . If x_i and y_i are a measurement in the EW channel, and the NS channel, respectively, then we define $x'_i = x_i \cos \phi_{\text{mag}} + y_i \sin \phi_{\text{mag}}$, and $y'_i = -x_i \sin \phi_{\text{mag}} + y_i \cos \phi_{\text{mag}}$. In this way the geomagnetic radiation contribution should be in the x' channel only. From these transformed measurements a parameter R is defined that is sensitive to deviations from geomagnetic polarized signal.

$$R_{\text{Sim}} = \frac{\sum_{i=1}^N x'_i y'_i}{\sum_{i=1}^N (x_i'^2 + y_i'^2)}. \quad (5)$$

With N , the number of samples in the signal window, and $i=1$ is the sample at the lower edge of the signal window. If the polarization of the radio signal is completely described by geomagnetic radiation, then $R=0$. To compare the noiseless simulations with the real measurements, an adjustment of R is needed to compensate for uncorrelated background.

$$R_{\text{Data}} = \frac{\sum_{i=1}^N x'_i y'_i}{\sum_{i=1}^N (x_i'^2 - n_x^2) + \sum_{i=1}^N (y_i'^2 - n_y^2)}. \quad (6)$$

In which n_x and n_y are the average noise levels, which can be derived in a noise window from the same time series. In Fig. 2, the dependence of R is shown as function of ϕ'_{obs} for the 494 events that were measured in coincidence with the SD. The electric field is calculated at various distances to probe the lateral behavior of the parameter R . An oscillation with a period of 360° is expected for the radial polarization of the charge-excess contribution. In case of the MGMR simulations this pattern is clearly visible for distances smaller than 300 m. For distance larger than 600 m there are some deviations, but the overall patterns still has a period of 360° . For the REAS3 simulations the polarization

³ In some literature different naming conventions are used, $Q=S_1$ and $U=S_2$.

Download English Version:

<https://daneshyari.com/en/article/1823938>

Download Persian Version:

<https://daneshyari.com/article/1823938>

[Daneshyari.com](https://daneshyari.com)